
PERGAMON

Journal of Quantitative Spectroscopy & Radiative Transfer 73 (2002) 461–472

Journal of Quantitative Spectroscopy & Radiative Transfer

www.elsevier.com/locate/jqsrt

Application of composition PDF methods in the investigation of turbulence–radiation interactions

Genong Li, Michael F. Modest *

Department of Mechanical Engineering, Pennsylvania State University, University Park, PA 16802, USA

Received 10 August 2001

Abstract

The composition probability density function (PDF) method is used to study radiating reactive flows. The method is able to treat turbulence–radiation interactions (TRI) in a rigorous way: many unclosed terms due to TRI in the traditional Reynolds-averaging process can be calculated exactly and all others can be accurately modeled by using the optically thin eddy approximation. The application of the method is demonstrated by considering a simplified methane/air diffusion flame, which shows enhancement of the radiative fluxes as a result of TRI. The importance of considering different TRI terms is investigated, indicating that the absorption coefficient–Plank function correlation is the most important. © 2002 Elsevier Science Ltd. All rights reserved.

Keywords: Turbulence–radiation interactions; PDF method; Correlated-k

1. Introduction

In order to predict radiative heat transfer accurately in many practical turbulent flows, it is necessary to couple the radiation calculation with turbulence calculations. This requires the solution of many coupled partial differential equations. In practice, these equations need to be Reynolds or Favre averaged. The difficulty comes in the averaging process: many unclosed terms appear as a result of turbulence–radiation interactions (TRI) and need to be modeled. Traditional moment methods fail to obtain closure for these terms because too many additional partial differential equations need to be modeled and solved simultaneously, which generally exceeds the power of current computers [1]. As a consequence, traditional modeling of radiating reactive flows has generally ignored TRI, i.e., radiation calculations have been based on mean temperature and concentration fields [2], although

* Corresponding author. Fax: +1-814-863-8682.
E-mail address: mfm6@psu.edu (M.F. Modest).

0022-4073/02/$ - see front matter
PII: S0022-4073(01)00218-7

experimental work has suggested that mean radiative quantities may differ significantly from those based on mean scalar values [3].

Some efforts have been made to couple radiation and turbulence calculations in a more rigorous way. Song and Viskanta [4] have investigated a turbulent premixed flame inside a two-dimensional furnace. While TRI were considered, in order to obtain closure for their governing equations correlation functions for gaseous properties had to be assumed. Gore et al. [5] and Hartick et al. [6] applied this approach to the study of diffusion flames, in which extended $k-\varepsilon-g$ models were used. To consider TRI, the shape of the probability density function of mixture fraction and total enthalpy had to be prescribed.

Mazumder and Modest [1] used the velocity–composition PDF method to investigate TRI. In their method, velocities, species concentrations and temperature were treated as random variables and the probability density function of these variables were considered. The uniqueness of this method is that it can resolve various interactions between turbulence, chemical reactions and radiative transfer. Using this method, Mazumder and Modest were able to calculate many unclosed terms due to TRI exactly. One of the disadvantages of this method is that its solution technique, the so-called PDF/Monte Carlo method, is relatively CPU intensive. In addition, the velocity–composition PDF method, although powerful in potential, is still at an early stage of development, making it difficult to apply to general 2D and 3D problems.

A similar approach, called the composition PDF method, will be used in this study, in which only species concentrations and temperature/enthalpy (called the composition variables, since they determine the composition of the mixture) are treated as random variables. The composition PDF method has been developed and successfully used in numerical simulations of nonradiating reactive flows [7]. The most remarkable feature of this method is that it can treat chemical reactions exactly—without resorting to any combustion model. It will be shown in this paper that, in radiating reactive flows, the composition PDF method is able to treat TRI more rigorously as well. The application of this method is illustrated by considering a simple methane/air diffusion flame.

2. Gas radiation calculations and TRI in radiation reactive flows

In a problem where thermal radiation is significant, the energy equation needs to include a radiative source term

$$S_{\text{radiation}} = -\nabla \cdot \underline{q}^{\text{R}} = -\int_0^\infty \kappa_\eta (4\pi I_{\text{b}\eta} - G_\eta)\,\mathrm{d}\eta, \quad G_\eta = \int_{4\pi} I_\eta\,\mathrm{d}\eta, \tag{1}$$

where $\underline{q}^{\text{R}}$ is the radiative heat flux vector; κ_η is the spectral absorption coefficient of the radiating gas, $I_{\text{b}\eta}$ is the spectral blackbody intensity (or Planck function), and G_η is the spectral incident radiation, which is the spectral radiation intensity I_η integrated over all solid angles.

One challenge in gas radiation calculations comes from the strong spectral dependence of radiation properties. Although line-by-line calculations can be used for best accuracy, such calculations are too time-consuming for any practical combustion system. Global methods such as the Weighted-Sum-of-Gray-Gases Model (WSGG) are commonly used [8]. Recently, the full-spectrum correlated-k distribution method (FSCK) has been developed by Modest and Zhang [9], and has been shown to be superior to the WSGG model, to which it reduces in its crudest implementation.

The method is exact within its limitations [gray walls, gray scattering properties, spectral absorption coefficient obeying the so-called scaling approximation, i.e., the spectral and spatial dependence of the absorption coefficient are separable $\kappa_\eta(\eta,\underline{\phi}) = k_\eta(\eta)u(\underline{\phi})$ where $\underline{\phi}$ are the composition variables] and will be used in this study.

In the FSCK method the spectrally dependent part of the absorption coefficient, k_η, which oscillates rapidly in spectral space, is reordered as a function of an equivalent fractional Planck function g (which is the cumulative distribution function of the absorption coefficient calculated over the whole spectrum and weighted by the Planck function). The advantage of the reordering is that k is much better behaved in g space (e.g., monotonically increasing and free of discontinuities). Generally, the reordered k also depends on temperature. However, in order to use arbitrary RTE solution techniques, a one-to-one correspondence between k and g is required. This is accomplished in the FSCK method by choosing a fixed reference temperature to obtain $k(g)$ and moving the temperature dependence to a weight function a (which is the ratio of the two k-distributions at the temperature of interest and at the reference temperature). As a result, the radiative heat source term can be rewritten as

$$S_{\text{radiation}} = -\int_0^1 k_g u(4\pi a_g I_\text{b} - G_g)\,\mathrm{d}g, \tag{2}$$

where the dependence of the variables has been changed from wavenumber η to fractional Planck function g. Since k is monotonically increasing and free of discontinuities, integration over g space is much simpler, needing far fewer points to represent the spectral features of gas radiation than would be required in unordered spectral space. In practical calculations, the integration is replaced by numerical quadrature. If Gaussian quadrature is used, Eq. (2) becomes

$$S_{\text{radiation}} \approx -\sum_{j=1}^{M} \omega_j k_j u(4\pi a_j I_\text{b} - G_j), \tag{3}$$

where M is the total number of quadrature points and the ω_j are the quadrature weights. The incident radiation G_j must be determined by solving the radiative transfer equation (RTE). Among the many solution techniques available, one of the simplest, yet very powerful method is the P_1 approximation, which reduces the equation of transfer from a very complicated integral equation to a relatively simple partial differential equation. For the vast majority of important engineering problems (i.e., in the absence of extreme anisotropy in the intensity filed), the method provides high accuracy at very reasonable computational cost. Furthermore, the P_1 approximation can easily be combined with sophisticated spectral models such as the FSCK method. Within the P_1 approximation, the incident radiation is governed by a Helmholtz equation, i.e. [10],

$$\nabla\cdot\left(\frac{1}{3k_j u}\nabla G_j\right) = k_j u G_j - 4\pi k_j u a_j I_\text{b}, \quad j = 1,\ldots,M, \tag{4}$$

subject to the boundary condition,

$$-\frac{2(2-\varepsilon)}{3\varepsilon}\hat{n}\cdot\nabla G_j = k_j u(4\pi a_j I_\text{b} - G_j), \tag{5}$$

where ε is the emittance and $\hat{n}$ is a unit normal at a boundary surface. The values of $k_j(g_j)$, $u(\underline{\phi})$ and $a_j(T,g_j)$ are obtained from a pre-calculated FSCK data base.

To couple radiation with flow calculations, the radiative source term and the P_1 equation need to be Reynolds averaged, leading to

$$\langle S\rangle_{\text{radiation}} \approx -\sum_{j=1}^{M} \omega_j k_j [4\pi\langle u a_j I_b\rangle - \langle u G_j\rangle], \tag{6}$$

$$\nabla\cdot\left[\frac{1}{3k_j}\left\langle\frac{1}{u}\nabla G_j\right\rangle\right] = k_j\langle u G_j\rangle - 4\pi k_j\langle u a_j I_b\rangle, \quad j=1,\ldots,M, \tag{7}$$

where Reynolds-averaged means are represented by angle brackets. As a result of TRI three terms, $k_j\langle u a_j I_b\rangle$, $k_j\langle u G_j\rangle$ and $\langle\nabla G_j/u\rangle$, representing correlations between dependent variables, need to be modeled. Different unclosed terms may arise in the Reynolds averaging process if different RTE solution techniques or different gas radiation models are used. However, all of them can be categorized into two groups: (a) correlations which can be calculated from the composition variables $\underline{\phi}$ only, and (b) correlations which cannot. Unclosed terms such as $k_j\langle u a_j I_b\rangle$ belong to group (a), since u, a_j and I_b all are functions of the composition variables only. Terms such as $k_j\langle u G_j\rangle$, $\langle\nabla G_j/u\rangle$ belong to group (b), because the G_j are not part of the composition space. Correlations in group (b) can be simplified for most practical turbulent reactive flows by using the optically thin eddy approximation as described by Kabashnikov and Myasnikova [11]. They suggested that the instantaneous local intensity of radiation is formed over a path traversing several turbulent eddies; therefore, it is only weakly correlated to the local radiative properties. The same argument holds for the local incident radiation, so that $k_j\langle u G_j\rangle \approx k_j\langle u\rangle\langle G_j\rangle$ and $\langle\nabla G_j/u\rangle \approx \nabla\langle G_j\rangle/\langle u\rangle$. As a result, all correlations needed to model TRI belong to group (a), which, as shown in the next section, can be calculated exactly using composition PDF methods.

3. Composition PDF methods

The philosophy of this approach is to consider the composition variables as random variables and to consider the transport of their PDF rather than their finite moments. The great advantage of this method is that the mean for any quantity Q, as long as it is a function of the composition variables only, such as chemical reaction source term $\langle S\rangle_{\text{reaction}}$, $k_j\langle u\rangle$, $k_j\langle u a_j I_b\rangle$, etc., can be evaluated directly from the PDF as

$$\langle Q\rangle = \int_0^\infty f(\underline{\psi}) Q(\underline{\psi})\,\mathrm{d}\underline{\psi}. \tag{8}$$

In this equation, $\underline{\psi}$ represents the sample space variables corresponding to the composition variables, $\underline{\psi} \equiv (\psi_1, \psi_2, \ldots, \psi_s)$ where s is the number of the composition variables (number of species plus the enthalpy) and the last variable in that set is reserved for enthalpy; and $f(\underline{\psi})$ is the probability density of the compound event $\underline{\phi} = \underline{\psi}$ (i.e., $\phi_1 = \psi_1, \phi_2 = \psi_2, \ldots, \phi_s = \psi_s$), so that

$$f(\underline{\psi})\,\mathrm{d}\underline{\psi} = \text{Probability}(\underline{\psi} \leqslant \underline{\phi} \leqslant \underline{\psi} + \mathrm{d}\underline{\psi}). \tag{9}$$

The composition PDF, $f(\underline{\psi})$, defined informally by Eq. (9), is the simplest form of the PDF methods, since it carries information of the composition variables only, and it is only a one-point probability

density function. However, since it contains all of the statistical information for the composition variables, its determination is more useful than that of the mean values in many ways. In a general turbulent reactive flow, the composition PDF is also a function of space, $\underline{x}$, and time, t. The transport equation for the composition PDF has been derived by Pope for nonradiating reactive flows [7]. For radiating reactive flows, the transport equation for the mass density composition PDF, $\mathscr{F}(\underline{\psi},\underline{x},t) = \rho(\underline{\psi},\underline{x},t)f(\underline{\psi},\underline{x},t)$, can be similarly derived, leading to

$$\frac{\partial \mathscr{F}}{\partial t} + \frac{\partial}{\partial x_i}[\tilde{u}_i \mathscr{F}] + \frac{\partial}{\partial \psi_\alpha}[S_{\text{reaction}}(\underline{\psi})\mathscr{F}]$$

$$= -\frac{\partial}{\partial x_i}[\langle u_i'' | \underline{\psi}\rangle \mathscr{F}] + \frac{\partial}{\partial \psi_\alpha}\left[\left\langle \frac{1}{\rho}\frac{\partial J_i^\alpha}{\partial x_i}\middle| \underline{\psi}\right\rangle \mathscr{F}\right] - \frac{\partial}{\partial \psi_s}[\langle S_{\text{radiation}}/\rho | \underline{\psi}\rangle \mathscr{F}], \tag{10}$$

where i and α are summation indices in physical space and composition space, respectively; and variables with tildes and double primes are the Favre means of the variables and the fluctuations about them, respectively. The notation of $\langle A|B\rangle$ is the expectation of the conditional probability of event A, given that event B occurs.

On the left-hand side of Eq. (10), the first two terms represent the rate of change of the PDF when following the Favre-averaged mean flow. The third term is the transport of the PDF in composition space by chemical reactions. The processes represented by these terms are accounted for exactly. In contrast, the terms on the right-hand side of Eq. (10) need to be modeled. The first two terms represent transport in physical space due to turbulent convection and transport in scalar space due to molecular mixing, respectively. They are usually modeled by using the gradient-diffusion hypothesis and a simple mixing model such as Dopazo's model [7], respectively, leading to

$$-\langle u_i'' | \psi\rangle \mathscr{F} \approx \Gamma_{\mathrm{T}} \frac{\partial \mathscr{F}}{\partial x_i}, \quad \left\langle \frac{1}{\rho}\frac{J_i^\alpha}{\partial x_i}\middle| \psi\right\rangle \approx \frac{1}{2} C_\phi \omega(\psi_\alpha - \tilde{\phi}_\alpha), \tag{11}$$

where $\Gamma_{\mathrm{T}} = c_\mu \langle\rho\rangle \sigma_\phi^{-1} k^2/\varepsilon$ is the turbulent diffusivity, and k, ε, c_μ and σ_ϕ are, respectively, the turbulent kinetic energy, dissipation rate of turbulent kinetic energy, a modeling coefficient in the standard k–ε turbulent model, and turbulent Schmidt or Prandtl numbers; finally, $\omega = \varepsilon/k$ is a turbulence 'frequency' and C_ϕ is a model constant.

The third term on the right-hand side of Eq. (10) represents the contribution from thermal radiation,

$$-\frac{\partial}{\partial \psi_s}[\langle S_{\text{radiation}}/\rho | \underline{\psi}\rangle \mathscr{F}] = \sum_{j=1}^{M} \omega_j \frac{\partial}{\partial \psi_s}[\langle k_j u(4\pi a_j I_{\mathrm{b}} - G_j)/\rho | \underline{\psi}\rangle \mathscr{F}]$$

$$= \sum_{j=1}^{M} 4\pi \omega_j k_j \frac{\partial}{\partial \psi_s}[(u a_j I_{\mathrm{b}}/\rho)\mathscr{F}] - \sum_{j=1}^{M} \omega_j k_j \frac{\partial}{\partial \psi_s}[\langle u G_j/\rho | \underline{\psi}\rangle \mathscr{F}]. \tag{12}$$

The first term on the right-hand side of the above equation represents radiative emission and can be considered exactly. The second term can be closed by adopting the optically thin eddy approximation, as discussed earlier. This leads to

$$\sum_{j=1}^{M} \omega_j k_j \frac{\partial}{\partial \psi_s}[\langle u G_j/\rho | \underline{\psi}\rangle \mathscr{F}] \approx \sum_{j=1}^{M} \omega_j k_j \frac{\partial}{\partial \psi_s}[(u\langle G_j\rangle/\rho)\mathscr{F}]. \tag{13}$$

As a result, the modeled transport equation for the composition mass density PDF can be written as

$$\frac{\partial \mathscr{F}}{\partial t} + \frac{\partial}{\partial x_i}[\tilde{u}_i \mathscr{F}] + \frac{\partial}{\partial \psi_\alpha}[S_{\alpha,\text{reaction}}(\underline{\psi})\mathscr{F}] - \sum_{j=1}^{M} 4\pi\omega_j k_j \frac{\partial}{\partial \psi_s}[(u a_j I_b/\rho)\mathscr{F}]$$

$$= \frac{\partial}{\partial x_i}\left[\Gamma_T \frac{\partial \mathscr{F}}{\partial x_i}\right] + \frac{1}{2} C_\phi \omega \frac{\partial}{\partial \psi_\alpha}[(\psi_\alpha - \tilde{\phi}_\alpha)\mathscr{F}] - \sum_{j=1}^{M} \omega_j k_j \frac{\partial}{\partial \psi_s}[(u\langle G_j\rangle/\rho)\mathscr{F}], \tag{14}$$

which is closed and contains all necessary information for all composition variables.

The composition PDF transport equation is a partial differential equation in $(4+s)$ dimensions. Traditional finite volume or finite element methods are very inefficient to solve an equation of such high dimensionality. Instead, the Monte Carlo method is generally used, in which the PDF is represented by a large number of computational particles. Each particle evolves in time and space according to a set of stochastic equations and carries with it all composition variables. The PDF is then obtained approximately as a histogram of the particles' properties in sufficiently small neighborhoods in physical space, and the mean quantities are deduced statistically by sampling the particles.

The composition PDF equation does not include any velocity field information. To determine velocities, turbulent diffusivity, turbulent time scales and incident radiation, which are required for the composition PDF equations, a flow solver has to be run in parallel with the PDF/Monte Carlo solver. A hybrid finite volume (FV)/PDF Monte Carlo method is used in this study, in which the velocity field $(\underline{\tilde{u}}, k, \varepsilon)$ and mean incident radiation $\langle G_i\rangle$ are solved by a finite volume code. This information is then transferred to the PDF Monte Carlo code, in which the composition variables (species concentrations and enthalpy) as well as functions of them (such as $\langle k_j u\rangle$ and $\langle k_j u a_j I_b\rangle$) are solved. In turn, the PDF Monte Carlo code supplies updated density and other information which is necessary for the solution of incident radiation for the finite volume code. The two codes are closely coupled and exchange information during every iteration. An efficient hybrid FV/PDF Monte Carlo method, which was developed by the present authors [12], will be used in the current study. This method uses time step splitting and particle splitting and combination techniques, allowing the PDF/Monte Carlo code to use any structured or unstructured grid system that is generated by the finite volume flow solver. For details the reader is referred to that paper.

4. Test problem

The numerical simulation of a simple diffusion flame in an axisymmetric combustor has been carried out to demonstrate the use of our model in the study of TRI. The same problem but in the absence of radiation has been considered previously by the same authors [12] during the development of an efficient hybrid FV/PDF Monte Carlo method. The problem is summarized here for the convenience of the reader.

The geometry of the combustor is shown in Fig. 1. A small nozzle at the center introduces methane at 80 m/s. Ambient air enters the combustor coaxially at 0.5 m/s. The overall equivalence ratio is approximately 0.76 (about 28% excess air). The high-speed methane jet initially expands with little interference from the outer wall, and entrains and mixes with the low-speed air. The

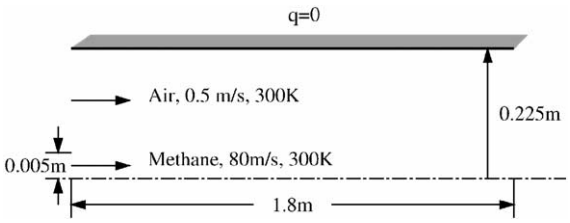

Fig. 1. Geometry of the cylindrical combustor.

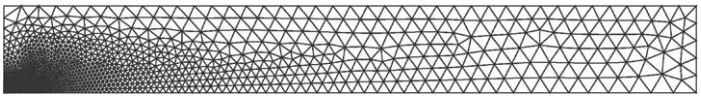

Fig. 2. The unstructured mesh used in the hybrid FV/PDF Monte Carlo method.

Reynolds number based on the methane jet diameter is approximately 28,000. Since the size of the fuel nozzle is very small, a lot of mesh points need be placed in the center region near the inlet. Two sets of unstructured meshes, one with 1247 nodes and 2317 cells and the other with 4753 nodes and 9103 cells were used to demonstrate grid-independence of the finite volume solution. The coarse mesh was employed for the solution of this problem, which is shown in Fig. 2. To obtain the flow field quantities, FLUENT [13] was used as the finite volume code, in which the standard k–ε model in conjunction with the use of wall functions were adopted. In the calculation, the pressure/velocity coupling was handled by the SIMPLE algorithm and convection terms were discretized by the second-order up-wind scheme. One key issue in the hybrid scheme is the passing of information between the two codes. The PDF/Monte Carlo technique is a statistical method and, hence, always has fluctuations associated with its solutions. If the level of these fluctuations is too high, it may cause divergence or other computational difficulties when information is communicated to the finite volume solver. Application of adaptive time step splitting and particle splitting and combination, which were developed earlier [12], keeps statistical fluctuations low and no divergence problems were observed in the finite volume code after the updated density field and coefficients for equations G_j were fed back from the PDF solver, even for low particle number densities, say 10 particles per cell on average. The conventional way to define residual error in the finite volume method is meaningless in the hybrid FV/PDF Monte Carlo simulation because the statistical error is generally larger than the truncation error. In the current study, the overall numerical error for a variable ϕ after the jth iteration is defined as $\mathrm{err} = 1/N \sum_{i=1}^{N} [\phi_i^j - \phi_i^{j-1}]^2/[\phi_i^{j-1}]^2$, where N is the total number of nodal points. This error never converges to zero, but rather to a value representative of the statistical fluctuation of the solution when steady state is reached. This level mainly depends on the number of particles in the simulation and on the number of steps, which it takes an average particle to cross the computational domain. If temperature is used to monitor the numerical error, a value on the order of 10^{-4} has been reached in the present calculation.

One of the strengths of the PDF approach is that multiple species and multiple-step chemistry can be easily incorporated without introducing any approximation, so that it can handle a wide range of combustion problems. But application of chemical kinetics requires to solve a set of stiff

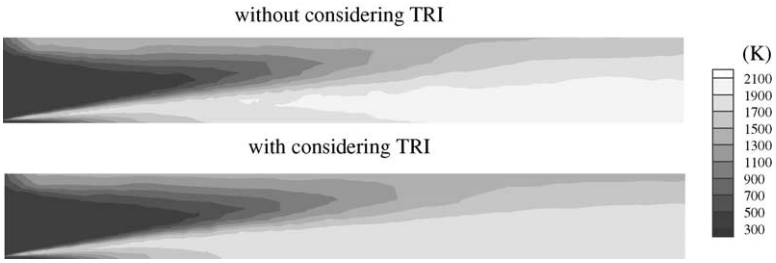

Fig. 3. Contours of equal temperatures.

ordinary differential equations for every particle during every iteration, which is extremely CPU time intensive. Thus, despite the apparent flexibility of the PDF method for describing complex chemistry in principle, as a first attempt to investigate such complex phenomena, the fast-chemistry assumption is employed in the current study to conserve CPU time, in which an infinitely fast chemical reaction rate is assumed at the particle level. While the fast-chemistry assumption has been used with great success in combustion modeling (e.g., in Bilger's flamelet model), it should be recognized that finite-rate effects may be very important in many practical applications, especially those involving flame ignition and/or extinction, or those involving predictions of minor species such as soot, NO and other radicals. In those circumstances, consideration of chemical kinetics is essential and radiation and turbulence are more closely coupled: TRI causes more emission, thus cooling down the flame; and a temperature decrease in the flame may dramatically change the chemical reaction rate, considering the strong nonlinearity of rate equations; this, in turn, changes the whole flame structure. As a result, TRI are expected to be much stronger for situations with "slow" reactions. This particular issue will be addressed in a follow-up paper [14]. In those situations, application of the fast-chemistry assumption will provide a lower-bound estimate of the importance of TRI.

To investigate the TRI, numerical experiments were done under two different scenarios. First, the problem was solved ignoring TRI, i.e., radiative properties as well as the Planck function were evaluated at cell mean values, $k_j\langle u\rangle \approx k_j u\langle\underline{\phi}\rangle$ and $k_j\langle ua_jI_b\rangle \approx k_j u\langle\underline{\phi}\rangle a_j(T)I_b(T)$. Then the problem was solved again considering turbulence–radiation interactions, i.e., the terms $k_j\langle u\rangle$ and $k_j\langle ua_jI_b\rangle$ were calculated exactly. Comparing the results from these two different scenarios, the most obvious difference is that the flame gets colder if TRI are considered. This can be observed from the temperature contours as shown in Fig. 3. The peak temperature in the computational domain decreases from 1985 to 1875 K. For this particular test problem, the difference of species concentration fields for the two different cases is not as large as that of the temperature field. This is caused by the use of the fast-chemistry assumption, in which chemical reaction rate is controlled by turbulent mixing only and, therefore, is not sensitive to temperature change. If more realistic chemical kinetics were incorporated the influence of TRI on concentration fields would be expected to be strong as well. Besides the temperature field change, radiation fields also change significantly as a result of TRI. Fig. 4 shows contours of the divergence of radiative heat flux, which indicates local radiative heat loss from the flame. From the figure it is seen that radiative heat loss is generally larger if turbulence–radiation interactions are considered in the calculations, especially in regions near the flame sheet where turbulent fluctuations are larger. The total radiative heat loss from the combustor increases from 22.0 to 29.1 kW (a 32% increase).

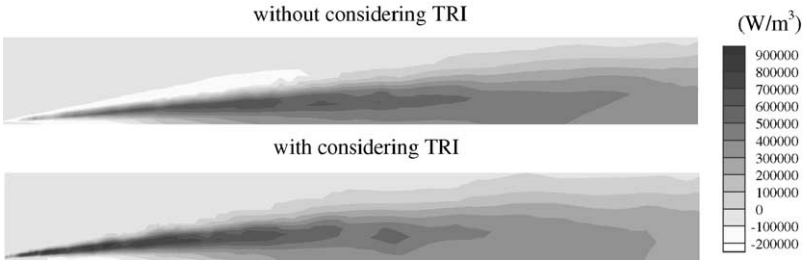

Fig. 4. Contours of equal $\nabla \cdot \underline{q}^{R}$.

Table 1
Approximations of two TRI terms for different scenarios

TRI term	No TRI	Partial TRI-1	Partial TRI-2	Partial TRI-3	Full TRI
$k_j\langle u\rangle$	$k_j\bar{u}$	$k_j\langle u\rangle$	$k_j\bar{u}$	$k_j\bar{u}$	$k_j\langle u\rangle$
$k_j\langle ua_jI_b\rangle$	$k_j\bar{u}\bar{a}_j\bar{I}_b$	$k_j\langle u\rangle\bar{a}_j\bar{I}_b$	$k_j\bar{u}\bar{a}_j\langle I_b\rangle$	$k_j\langle ua_jI_b\rangle$	$k_j\langle ua_jI_b\rangle$

Since radiation and turbulence calculations are closely coupled, considering TRI completely changes profiles of the composition variables. Therefore, a direct comparison sometimes may be misleading. The role of TRI on radiative heat transfer can be better understood by isolating their effects on the radiation calculations alone. This can be done by freezing the particle field (including particles' locations, particles' species concentrations and their temperatures) at a point in time, and then calculating radiation fields by ignoring TRI and considering TRI, respectively. To illuminate different facets of TRI, three intermediate scenarios are also considered. Together with the case of ignoring TRI and fully considering TRI, there are five scenarios to be investigated, namely no-TRI, partial TRI-1, partial TRI-2, partial TRI-3 and full-TRI as summarized in Table 1, where quantities evaluated simply from the mean composition variables are denoted with an overline. In TRI-1 only the absorption coefficient self-correlation is considered, with the weighted Planck function evaluated at mean property values; in TRI-2 only the influence of TRI on the mean Planck function is considered (sometimes referred to as 'temperature self-correlation'); and in TRI-3, the effects of absorption coefficient–Planck function correlation on emission are also included (but not on absorption). The particle field of the fully converged solution for the full-TRI case was used for this comparison, and Table 2 shows the overall energy balance, i.e., the calculated radiative heat loss from the combustor and the calculated radiative heat fluxes through its three boundaries. Compared with the radiative heat loss for the no-TRI case, the absorption coefficient self-correlation (TRI-1) does not show any significant impact, indicating that this is not an important issue. This is expected, since the absorption coefficient is linearly dependent on species concentrations and almost linearly dependent on temperature, so that $k_j\langle u\rangle$ is close to $k_j\bar{u}$, making the partial TRI-1 case similar to the no-TRI case. On the other hand, the effect of temperature self-correlation (TRI-2) is important, increasing the radiative source by about 30%. Thus, ignoring the temperature self-correlation (embodied in $\langle I_b\rangle$) is generally unacceptable because of the strongly nonlinear temperature-dependence of the Planck function. But, comparison with the full-TRI case shows that consideration of the temperature self-correlation alone

Table 2
The computed total radiative heat loss from the combustor and the computed total radiative heat fluxes through the boundaries

Different scenario	$\int\int\int \nabla \cdot \underline{q}^{R}\, dV$	$\int\int \hat{n} \cdot \underline{q}^{R}\, dS$ (kW)		
	(kW)	Inlet	Wall	Exit
No TRI	17.7	71.9	29.8	−84.0
Partial TRI-1	17.6	71.8	29.7	−83.9
Partial TRI-2	23.6	75.5	33.2	−85.1
Partial TRI-3	32.3	75.0	42.8	−85.5
Full TRI	29.1	74.9	39.7	−85.5

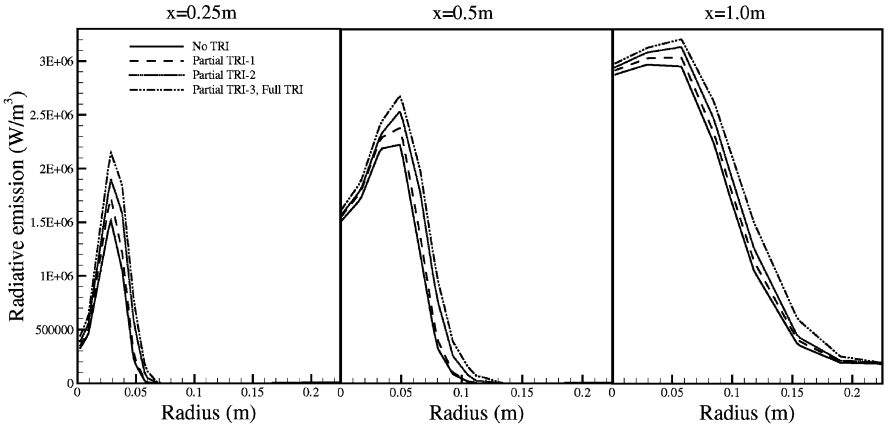

Fig. 5. Profiles of gaseous emission at different cross-sections.

is not sufficient. Including the absorption coefficient–Planck function correlation raises the radiative source another 50%; 20% of that are recovered by also considering the effects of absorption coefficient self-correlation on absorption (full TRI). To examine the differences in more detail, profiles of the flame emission and radiative heat loss at three cross-sections are shown in Figs. 5 and 6. Fig. 5 shows that radiative emission is always enhanced by TRI. Absorption is also enhanced as a result of TRI, but it cannot make up for the increase of emission, especially in regions near the flame sheet; consequently, the radiative heat loss from the flame increases as shown in Fig. 6. In regions that contain the flame sheet and where turbulent fluctuations are large, such as the cross-section at $x = 0.25$ m, emission and radiative heat loss increase by more than 30% if full turbulence–radiation interactions are considered. Comparison of profiles for different scenarios gives the same trend as that for total radiative heat loss: results of the no-TRI case are close to those of TRI-1, and results from TRI-3 are close to those from the full TRI case, while results from TRI-2 fall between those from the no-TRI and full TRI cases.

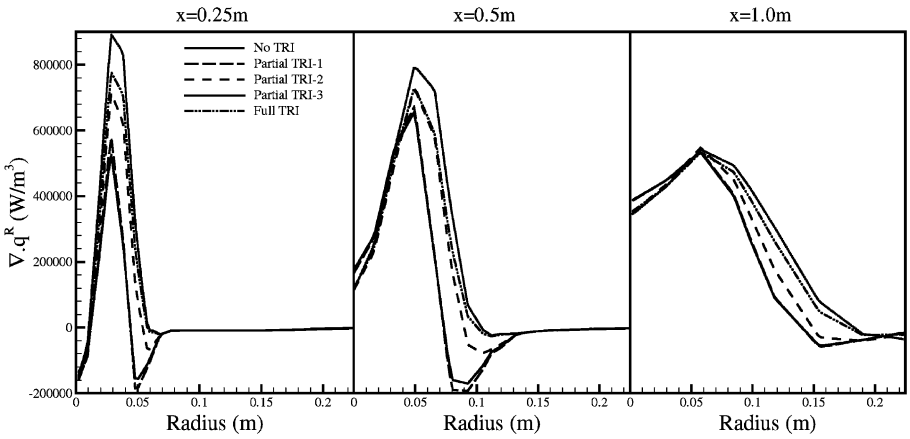

Fig. 6. Profiles of radiative heat loss at different cross-sections.

5. Conclusions

The composition PDF method has been formulated to include effects of turbulence–radiation interactions in a rigorous fashion. The use of this method in the study of TRI was demonstrated by considering a simple methane/air diffusion flame in a cylindrical combustor. The calculations show that, by ignoring turbulence–radiation interactions, the radiative heat loss is always underpredicted and, consequently, temperature levels are generally overpredicted. Through freezing a particle field, the importance of different TRI-related terms was illuminated. The absorption coefficient–Planck function correlation was found to be more important than other correlations and needs to be calculated accurately in order to determine turbulence–radiation interactions. Although nonlinearity of the Planck function on temperature is the severest among other functions, accurate determination of the temperature self-correlation alone appears insufficient.

Acknowledgements

The authors are grateful to the National Science Foundation for funding of this research under Grant Number CTS-9732223. The authors also want to thank Ms. H. Zhang for providing the FSCK data base for radiation calculations.

References

[1] Mazumder S, Modest MF. A PDF approach to modeling turbulence–radiation interactions in nonluminous flames. Int J Heat Mass Transfer 1998;42:971–91.
[2] Viskanta R. Overview of convection and radiation in high temperature gas flows. Int J Eng Sci 1998;36:1677–99.
[3] Faeth GM, Gore JP, Shuech SG, Jeng SM. Radiation from turbulent diffusion flames. Ann Rev Numer Fluid Mech Heat Transfer 1989;2:1–38.
[4] Song TH, Viskanta R. Interaction of radiation with turbulence: application to a combustion system. J Thermophys 1987;1(1):56–62.

[5] Gore JP, Ip US, Sivathanu YR. Coupled structure and radiation analysis of acetylene/air flames. J Heat Transfer 1992;114:487–93.
[6] Hartick JW, Tacke MT, Fruchtel G, Hassel EP, Janicka J. Interaction of Turbulence and Radiation in Confined Diffusion Flames, Twenty-Sixth Symposium (International) on Combustion 1996; 26:75–82.
[7] Pope SB. PDF methods for turbulent reactive flows. Progr Energy Combust Sci 1985;11:119–92.
[8] Hottel HC, Sarofim AF. Radiative transfer. New York: McGraw-Hill, 1967.
[9] Modest MF, Zhang H. The full-spectrum correlated-k distribution for thermal radiation from molecular gas-particulate mixtures. ASME J Heat Transfer 2002 (1), in press.
[10] Modest MF. Radiative heat transfer. New York: McGraw-Hill, 1993.
[11] Kabashnikov VP, Myasnikova GI. Thermal radiation in turbulent flows—temperature and concentration fluctuations. Heat Transfer-Sov Res 1985;17(6):116–25.
[12] Li G, Modest MF. An effective particle tracing scheme on structured/unstructured grids in hybrid finite volume/PDS Monte Carlo methods. J Comput Phys 2001;173:187–207.
[13] FLUENT. Computational fluid dynamics software, Version 5, 1998.
[14] Li G, Modest MF. Investigation of turbulence–radiation interaction in reacting flows using a hybrid FV/PDF method. 2002, in preparation.